Protonated Polycyclic Aromatic Nitrogen Heterocyclics: Proton Affinities, Polarizabilities, Atomic and Ring Charges of 1−5 Ring Ions.

ARTICLE *in* THE JOURNAL OF PHYSICAL CHEMISTRY A · DECEMBER 2014

Impact Factor: 2.69 · DOI: 10.1021/jp5069939 · Source: PubMed

3 AUTHORS, INCLUDING:

Michael Noah Mautner
Virginia Commonwealth University
202 PUBLICATIONS **5,207** CITATIONS

THE JOURNAL OF PHYSICAL CHEMISTRY A

Article

pubs.acs.org/JPCA

Protonated Polycyclic Aromatic Nitrogen Heterocyclics: Proton Affinities, Polarizabilities, and Atomic and Ring Charges of 1−5-Ring Ions

Robert G. A. R. Maclagan,*[,†] Scott Gronert,[‡] and Michael Meot-Ner (Mautner)[†,‡]

[†]Department of Chemistry, University of Canterbury, Christchurch 8001, New Zealand

[‡]Department of Chemistry, Virginia Commonwealth University, Richmond Virginia 23284-2006, United States

Supporting Information

ABSTRACT: Calculated proton affinities, polarizabilities, and some ionization energies and atomic and ring NBO charges are reported for 31 polycyclic aromatic nitrogen heterocyclics (PANHs) with 1−5 rings, calculated on the on the M06-2X/6-311+g**//B3LYP/6-31g* level of theory. The calculated proton affinities from 226 to 241 kcal mol^{-1} for 3−5-ring compounds, predict well the relative experimental values. The proton affinities increase with increasing molecular size and show a linear correlation with polarizabilities. Linear geometry and nitrogen located in the central ring also favor increased proton affinity. These trends estimate a PA > 241 kcal mol^{-1} for an infinite linear chain, end-ring-N PANH molecule, and >261 kcal mol^{-1} for an edge-N-doped graphene sheet, making it a superbase. NBO analysis shows that from pyridineH$^+$ to large 5-ring ions, the N−H nitrogen carries a constant q(N) = −0.46 ± 0.1 charge, and the N−H hydrogen a constant q(H) = 0.43 ± 0.01 positive charge, similar to the q(H) in NH_4^+. Overall, the NH group is nearly electrically neutral, and a nearly full positive charge is distributed on the aromatic hydrocarbon rings of the ions. When the nitrogen is in a central ring, that ring is negative, and the positive ionic charge is delocalized toward the end rings. When the nitrogen is in an end ring, the ionic charge is distributed more evenly. Increasing proton affinities with increasing polarizability result not from increasing charge transfer from the proton to the aromatic rings, but from increasing delocalization of the transferred charge in the aromatic hydrocarbon rings of the ions. In two-nitrogen compounds, interactions between the ring nitrogens decrease the proton affinities, but this effect decreases in larger ions.

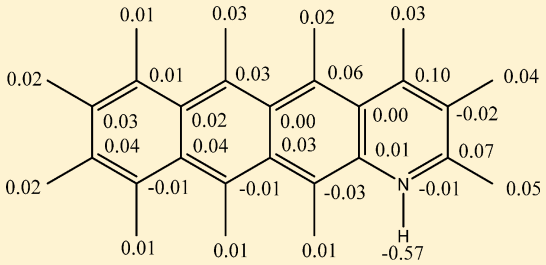

1. INTRODUCTION

Polycyclic aromatic nitrogen heterocyclic hydrocarbons (PANHs) are found in natural and industrial environments including coal tar, combustion products, dyes, biological compounds, and meteorites.[1−3] PANHs are also considered to be N-doped counterparts of interstellar polycylic aromatic hydrocarbons (PAHs), identified by a 6.2 μM emission band, suggesting that 1%−2% of cosmic nitrogen is contained in PANH compounds, if present.[4,5] In fact, statistically by cosmic C/N ratios alone, most interstellar polycyclic aromatics should contain ring nitrogens.

PANH compounds can be ionized or protonated in low pH solutions in biological systems and in ices,[6] in the gas phase in mass spectrometry and combustion, and in interstellar clouds, where emission bands of ionized PANHs at 6.3−6.5 μm have been indicated.[7,8] PANHs have high intrinsic basicities (GB) and proton affinities (PA), making them potential proton sinks in gas-phase environments. The large planar ions can then serve as nucleation centers for clusters and ices and provide catalytic molecular surfaces for associative charge (ACT) or associative proton transfer (APT) reactions.[9−11]

PANHs also model structural units of ionized and protonated N-doped graphene. Trends in their properties with increasing size may be extrapolated to ionized edge-N-doped graphene, similar to extrapolation from PAHs to ionized graphene and graphite.[12,13]

With these various roles, the ion energetics of PANHs have broad significance. However, few data exist on the energetics of unsubstituted PANH ions. Gas-phase basicities and proton affinities are available for substituted pyridine derivatives,[14−17] but only for a few small unsubstituted PANHs, mostly from early mass spectrometric equilibrium measurements.[12−19] This scarcity of information is due in part to the unavailability of materials and to their low vapor pressures, which prevent mass spectrometric equilibrium studies.

These compounds are also demanding theoretically because high-level calculations are possible only for small 1- and 2-ring PANH compounds. In this paper, we apply DFT calculations to all the PANHs with one nitrogen atom and 1−3 aromatic rings, some selected 4−5-ring compounds, and some representative two-nitrogen compounds.

Received: July 15, 2014
Revised: December 4, 2014
Published: December 5, 2014

DOI: 10.1021/jp5069939
J. Phys. Chem. A 2015, 119, 127−139

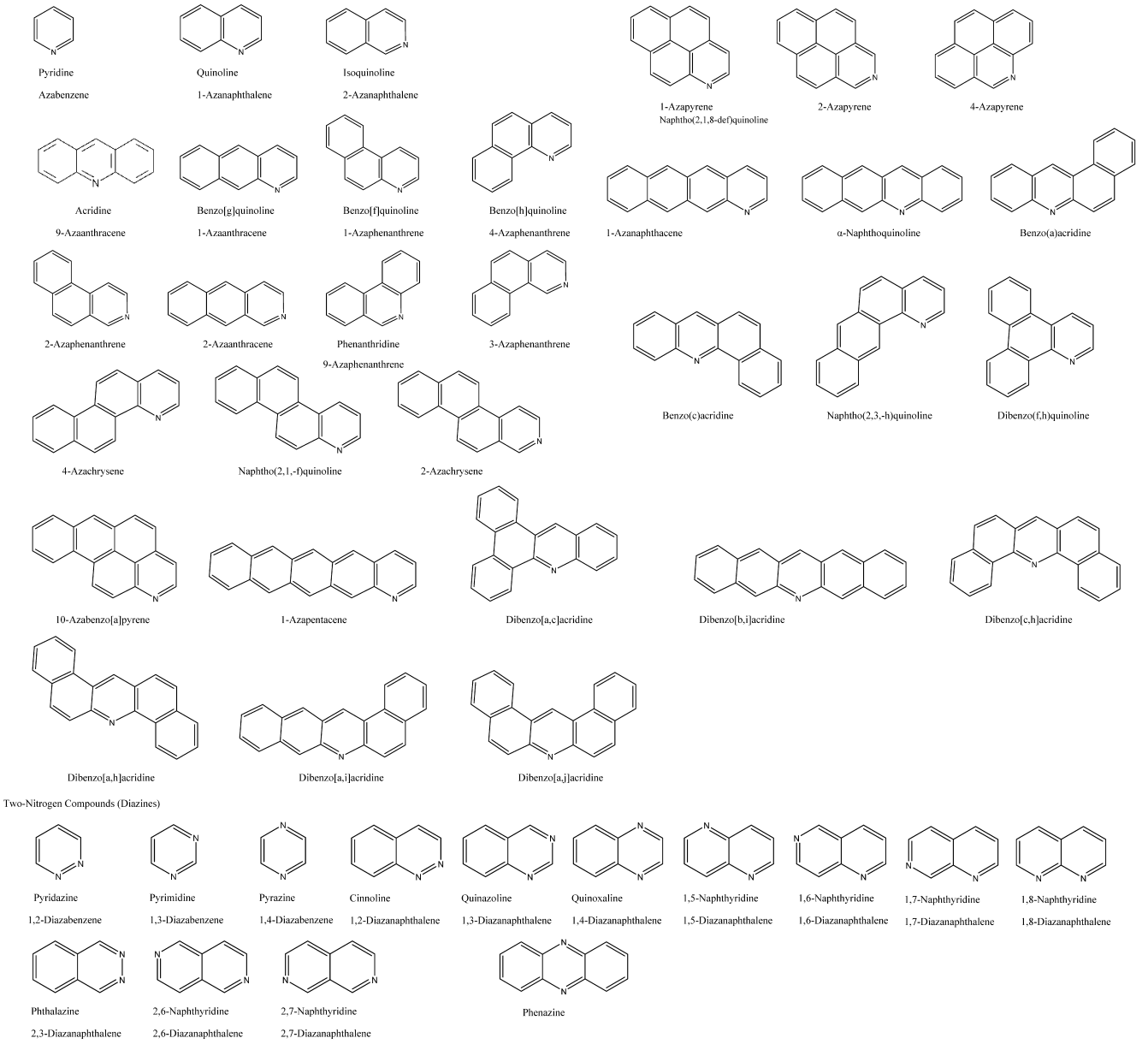

Figure 1. Structures of N heterocyclics.

2. COMPUTATIONAL METHODS

The structure of the PANHs and their protonated ions that are reported in the NIST Chemistry Webbook,[18,19] plus other selected PANH structures,[20] shown in Figure 1, were optimized at the B3LYP/6-31G* level of theory.

Where comparison is made with experimental values, these are taken from the NIST Webbook,[18,19] based on equilibrium data,[21−27] and from our recent experiments.[20]

This level of theory was chosen as it is computationally efficient, allows treatment of large molecules, and provides reasonably reliable geometries.[28] B3LYP/6-31G* geometries are used in the G3(MP2)B3 method.[29] Initial single point calculations using these geometries were then performed at the B3LYP/6-311+g** level of theory. Calculations by Leito et al. showed that this basis set gives reasonably accurate gas-phase basicities for superbases in the upper PA range.[30−32] We also performed calculations using the B3LYP/aug-cc-pvdz and B3LYP/aug-cc-pvtz basis sets. Because the use of the B3LYP functional did not perform as well for 3−5-ring compounds as it did for 1−2-ring compounds the calculations were repeated with the M06-2X functional. Calculations were also performed at the MP2/6-311+G** level of theory. All enthalpies calculated are at 298 K with the zero point vibrational energy contributions corrected by a factor 0.96.

3. RESULTS AND DISCUSSION

In this paper we report calculations on nitrogen heterocyclics containing a single nitrogen atom, and some containing two nitrogen atoms for comparison. Measurements and calculations on further compounds with two or more nitrogen atoms will be reported separately.

3a. Protonation Thermochemistry. The gas-phase basicity and proton affinity correspond to the enthalpy and free energy reaction 1, respectively, where PA = $-\Delta H^{\circ}_1$, GB = $-\Delta G^{\circ}_1$, and $S_{prot} = S(BH^+) - S(B)$ calculated here at 298 K using M06-2X/6-311+G**//B3LYP/6-31G*, B3LYP/6-311+G**//B3LYP/6-31G*, and MP2/6-311+G**//B3LYP/6-31G* levels of theory.

DOI: 10.1021/jp5069939
J. Phys. Chem. A 2015, 119, 127−139

Table 1. Calculated Thermodynamic Properties of 1−5-Ring PANH Compounds: Proton Affinities (PA), Gas-Phase Basicities (GB), and Protonation Entropies[a]

		exp	M06-2X		B3LYP		MP2			
formula	molecule	PA[b]	PA[c]	ΔPA[d]	PA[c]	ΔPA[d]	PA[c]	ΔPA[d]	GB[a]	S_{prot}[e]
C_5H_5N	pyridine	222.2	220.3	−1.9	223.7	1.5	219.5	−2.7	212.3	0.4
C_9H_7N	quinoline	227.8	225.7	−2.1	229.8	2.0	223.9	−3.9	217.7	0.6
	isoquinoline	227.5	226.3	−1.2	230.4	2.9	225.2	−2.3	218.3	0.5
$C_{13}H_9N$	acridine	232.4	232.3	−0.1	236.6	4.2	228.7	−3.7	224.4	0.7
	benzo[*g*]quinoline		229.0		233.6				221.1	0.7
	benzo[*f*]quinoline	228.6	228.5	−0.1	233.1	4.5	226.7	−1.9	220.5	0.6
	benzo[*h*]quinoline	228.0	226.3	−1.7	231.0	3.0	225.2	−2.8	218.5	1.2
	2-azaphenanthrene		228.6		233.3				220.6	0.7
	phenanthridine	228.5	228.4	−0.1	233.0	4.5	226.7	−1.8	220.4	0.6
	2-azaanthracene		229.9		234.7				221.9	0.6
	3-azaphenanthrene		229.1		233.8				221.1	0.7
$C_{15}H_9N$	1-azapyrene		233.8		238.6				225.8	0.7
	2-azapyrene		230.3		235.3				222.3	0.5
	4-azapyrene		228.9		233.6				220.9	0.6
$C_{17}H_{11}N$	1-azanaphthacene		231.2	-	236.2				223.2	0.7
	α-naphthoquinoline		236.5		240.9				228.5	0.7
	benzo(*a*)acridine	234.2	233.9	−0.3	238.7	4.5	230.7	−3.5	226.0	0.7
	benzo(*c*)acridine	232.5	231.6	−0.9	236.4	3.9	229.1	−3.4	223.8	1.3
	naphtho(2,3-*h*)quinoline		228.0		233.2				220.3	1.3
	dibenzo(*f*,*h*)quinoline	228.9	227.5	−1.4	232.6	3.7	226.5	−2.4	219.9	1.9
	4-azachrysene		227.8		232.9				225.2	1.5
	naphtho(2,1-*f*)quinoline		230.5		234.6				226.7	0.7
	2-azachrysene		230.1		235.1				227.2	1.0
$C_{19}H_{11}N$	azabenzo[*a*]pyrene		235.9		241.2				233.3	0.9
$C_{21}H_{13}N$	1-azapentacene		232.7		238.0				224.8	0.9
	dibenzo[*a*,*c*]acridine		232.1		237.4				224.5	1.9
	dibenzo[*a*,*h*]acridine		233.0		238.3				225.2	1.2
	dibenzo[*a*,*i*]ac ridine		237.3		242.2				229.4	0.8
	dibenzo[*a*,*j*]acridine		235.2		240.4				227.2	0.6
	dibenzo[*b*,*i*]acridine		241.2		245.7				233.3	0.9
	dibenzo[*c*,*h*]acridine	233.0	230.8	−2.2	236.2	3.2	229.5	−3.5	223.6	3.2
$C_4H_4N_2$	1,2-diazine	216.8	216.6	−0.2	219.9	3.1	216.5	−0.3	211.7	0.2
	1,3-diazine	211.7	209.8	−1.9	213.0	1.3	208.3	−3.4	205.0	0.6
	1,4-diazine	209.6	206.8	−2.8	210.2	0.6	207.0	−2.6	211.7	0.5
$C_8H_6N_2$	cinnoline N1	223.8	222.8	−1.0	227.1	3.3	222.3	−1.5	214.7	0.4
	N2		223.9		228.3		223.9		215.7	0.3
	quinazoline N1		217.9		221.8		215.2		209.9	0.7
	N3		217.9		222.1		216.3		209.9	0.6
	quinoxaline	216.0	214.0	−2.0	218.4	2.4	213.5	−2.5	206.0	0.6
	1,5-naphthyridine		219.9		223.8		218.5		211.9	0.6
	1,6-naphthyridine N1		218.5		222.3		215.8		210.6	0.7
	N6		222.0		225.8		220.5		214.0	0.6
	1,7-naphthyridine N1		217.1		221.1		215.9		209.1	0.6
	N7		222.8		226.6		222.1		214.7	0.5
	1,8-naphthyridine		227.6		231.2		225.3		219.5	0.4
	2,3-naphthyridine		226.0		230.1		225.3		214.0	0.2
	2,6-naphthyridine		218.0		222.0		217.7		210.0	0.6
	2,7-naphthyridine		219.4		223.2		217.6		211.4	0.6
$C_{12}H_8N_2$	phenazine	224.3	221.9	−2.4	226.7	2.4	219.5	4.8	214.0	0.7

[a]Comparisons with experimental values are given where available. GB and PA in kcal mol^{-1}, S_{prot} in cal mol^{-1} K^{-1}. [b]Experimental value for pyridine, average of 222.2, 222.8, 222.2, and 221.8 kcal mol^{-1} from refs 21−27, and for other PANH compounds from evaluated data from refs 18 and 19, and from our measurements (ref 20). [c]This work, computational PAs at 298 K. [d]Difference ΔPA = $PA_{calc} - PA_{exp}$ (kcal/mol). [e]Computational $S_{prot} = S(BH^+) - S(B)$ at 298 K.

$$B_g + H_g^+ \rightarrow BH_g^+ \quad (1)$$

$$GB(B) = PA(B) + TS_{prot}(B) - TS(H^+) \quad (2)$$

For some compounds comparison is possible with experimental values. For the one and two-ring compounds pyridine, quinoline, and isoquinoline, the computed B3LYP PAs are higher by 1.5, 2.0, and 2.9 kcal/mol than the experimental (NIST)

DOI: 10.1021/jp5069939
J. Phys. Chem. A 2015, 119, 127−139

Table 2. Calculated Gas-Phase Ionization Energies (IE) of 1−5-Ring PANH Compounds[a]

		exp	M06-2X		B3LYP	
Formula	molecule	IE[a]	IE[b]	ΔIE[c]	IE[b]	ΔIE[c]
C_5H_5N	pyridine	213.5	222.3	8.8	218.8	5.3
C_9H_7N	quinoline	199.0	199.3	0.3	193.2	−5.8
	isoquinoline	196.7	197.6	0.9	191.4	−5.3
$C_{13}H_9N$	acridine	179.9	182.6	2.7	174.6	−5.3
	benzo[*g*]quinoline	175.3	177.5	2.2	171.1	−4.2
	benzo[*f*]quinoline	187.7	189.6	1.9	181.9	−5.8
	benzo[*h*]quinoline	185.4	186.7	1.3	179.4	−6.0
	2-azaphenanthrene		188.2		181.7	
	phenanthridine	191.6	192.7	1.1	185.2	−6.5
	2-azaanthracene		179.0		172.3	
	3-azaphenanthrene		192.7		185.1	
$C_{15}H_9N$	1-azapyrene		181.9		174.6	
	2-azapyrene		177.6		170.9	
	4-azapyrene		179.1		172.2	
$C_{17}H_{11}N$	1-azanaphthacene		163.5		156.9	
	α-naphthoquinoline		167.2		159.8	
	benzo(*a*)acridine		181.4		172.1	
	benzo(*c*)acridine		179.2		170.5	
	naphtho(2,3-*h*)quinoline		171.9		164.2	
	dibenzo(*f*,*h*)quinoline		186.1		177.3	
	4-azachrysene		178.2		170.6	
	naphtho(2,1-*f*)quinoline		182.6		173.0	
	2-azachrysene		181.4		173.4	
$C_{19}H_{11}N$	azabenzo[*a*]pyrene		172.6		165.2	
$C_{21}H_{13}N$	1-azapentacene		153.6		147.0	
	dibenzo[*a*,*c*]acridine		180.9		170.4	
	dibenzo[*a*,*h*]acridine		176.5		167.1	
	dibenzo[*a*,*i*]ac ridine		167.4		159.0	
	dibenzo[*a*,*j*]acridine		180.4		170.7	
	dibenzo[*b*,*i*]acridine		153.5		150.3	
	dibenzo[*c*,*h*]acridine		178.8		168.3	
$C_4H_4N_2$	1,2-diazine	201.6	201.5	−0.1	197.6	−4.0
	1,3-diazine	215.2	225.5	10.3	217.5	2.3
	1,4-diazine	214.2	224.7	10.5	217.0	2.8
$C_8H_6N_2$	cinnoline	196.3	191.9	−4.4	186.8	−9.5
	quinazoline	208.0	208.6	0.6	203.2	−4.8
	quinoxaline	207.8	208.8	1.0	199.8	−8.0
	1,5-naphthyridine	212.2	216.0	3.8	209.7	−2.5
	1,6-naphthyridine	209.2	208.7	−0.5	202.8	−6.4
	1,7-naphthyridine	207.3	207.4	0.1	202.0	−5.3
	1,8-naphthyridine	212.2	210.0	1.2	200.4	−11.8
	2,3-naphthyridine	193.7	193.9	0.2	188.6	−5.1
	2,6-naphthyridine	204.6	205.1	0.5	199.6	−5.0
	2,7-naphthyridine	207.1	208.2	1.1	202.1	−5.0
$C_{12}H_{10}N_2$	phenazine	192.1	192.8	0.7	183.8	−8.3

[a]Experimental values from Hunter and Lias, 1998, and NIST Webbook June 2014, ref 19, based on data in ref 15. [b]This work, computational IEs at 298 K. [c]Difference ΔIE = IE_{calc} − IE_{exp} (kcal/mol)

values. The difference continues to increase with molecular size, and for the 3−5-ring compounds in the companion paper,[20] the computed PAs are higher than experiment by an about constant 3.9 ± 0.6 kcal/mol. Calculations using the aug-cc-pvdz basis set for 13 compounds yielded PAs similar to the B3LYP/6-311+G**//B3LYP/6-31G* results shown in Table 1, with an average difference of 0.26 ± 0.28 kcal/mol, and largest difference of 0.7 kcal/mol. We also performed aug-cc-pvtz calculations, which gave PA values somewhat still higher and more different from experiment than aug-cc-pvdz, whereas calculations at the MP2 level gave lower PA values and in poorer agreement with experiment. Calculations at the M06-2X/6-311+G**/B3LYP/6-31G* gave better agreement, being on average 0.85 ± 0.83 kcal/mol less than experiment for 3−5-ring compounds. Calculations at the MP2 level gave lower PA values on average 2.9 ± 0.7 kcal/mol less than experiment for 3−5-ring compounds.

Considering that the B3LYP computational PAs are higher by 3.9 ± 0.6 kcal mol^{-1} than experiment for the measured 3−5-ring compounds,[20] we recommend PA and GB values for the 3−5-ring compounds in Table 1 that are adjusted higher by 1.1 kcal/mol from the M06-2X values or lower by 3.9 kcal/mol than the calculated B3LYP values. The two sets of values adjusted this way

DOI: 10.1021/jp5069939
J. Phys. Chem. A 2015, 119, 127−139

Table 3. Calculated Theoretical Proton Affinities of One-Nitrogen Heterocyclics, Correlation with Polarizability and Deviations from the Correlation, and Calculated Polarizabilities, Dipole Moments, and N−H Bond Lengths[a]

					theory		
		PA theory[b]	PA linear reg[c]	PA dev[d]	polarizability[e]	dipole moment[f]	R(N−H)[g]
C_5H_5N	pyridine	220.3	223.2	2.9	7.5	2.38	1.018
C_9H_7N	quinoline	225.7	225.6	−0.1	13.9	2.17	1.017
	isoquinoline	226.3	225.7	−0.6	14.0	2.73	1.016
$C_{13}H_9N$	acridine	232.3	228.7	−3.6	22.2	2.01	1.016
	benzo[*g*]quinoline	229.0	228.7	−0.3	22.2	2.15	1.016
	benzo[*f*]quinoline	228.5	228.2	−0.3	20.9	2.28	1.017
	benzo[*h*]quinoline	226.3	228.3	2.0	21.1	1.75	1.015
	2-azaphenanthrene	228.6	228.2	−0.4	20.8	3.00	1.016
	phenanthridine	228.4	228.2	−0.2	20.9	2.44	1.017
	2-azaanthracene	229.9	228.6	−1.3	21.9	3.04	1.015
	3-azaphenanthrene	229.1	228.2	−0.9	20.8	2.81	1.016
$C_{15}H_9N$	1-azapyrene	233.8	229.5	−4.3	24.4	2.75	1.015
	2-azapyrene	230.3	229.5	−0.8	24.3	2.96	1.016
	4-azapyrene	228.9	229.6	0.7	24.5	2.39	1.017
$C_{17}H_{11}N$	1-azanaphthacene	231.2	232.3	1.1	32.0	2.17	1.016
	α-naphthoquinoline	236.5	232.3	−4.2	32.0	2.01	1.015
	benzo(*a*)acridine	233.9	231.6	−2.3	29.9	2.10	1.016
	benzo(*c*)acridine	231.6	231.6	0.0	29.9	1.59	1.014
	naphtho(2,3-*h*)quinoline	228.0	231.6	3.6	30.0	1.58	1.015
	dibenzo(*f*,*h*)quinoline	227.5	230.7	3.2	27.6	1.84	1.014
	4-azachrysene	227.8	231.1	3.3	28.7	1.77	1.014
	naphtho(2,1-*f*)quinoline	230.5	231.2	0.7	28.9	2.97	1.015
	2-azachrysene	230.1	231.1	1.0	28.6	3.20	1.015
$C_{19}H_{11}N$	10-azabenzo[*a*]pyrene	235.9	232.8	−3.1	33.3	2.86	1.014
$C_{21}H_{13}N$	1-azapentacene	232.7	236.6	3.9	43.4	2.19	1.016
	dibenzo[*a*,*c*]acridine	232.1	234.1	2.0	36.6	1.66	1.014
	dibenzo[*a*,*h*]acridine	233.0	234.7	1.7	38.3	1.67	1.014
	dibenzo[*a*,*i*]acridine	237.3	235.5	−1.8	40.6	2.09	1.015
	dibenzo[*a*,*j*]acridine	235.2	234.4	−0.8	37.6	2.12	1.016
	dibenzo[*b*,*i*]acridine	241.2	236.6	−4.6	43.5	2.02	1.014
	dibenz[*c*,*h*]acridine	230.8	234.4	3.6	37.5	1.25	1.012

[a]PA in kcal/mol, polarizabilities in Å^3, dipole moments in Debye. [b]Proton affinities from M06-2X/6-311+G**//B3LYP/6-31G* theory calculations. [c]Proton affinities calculated from linear regression of Figure 3. [d]Difference between PA from theory and from the linear regression fits. [e]Polarizabilities from B3LYP/6-31G* calculations. For comparison, the experimental polarizability of pyridine is 9.49 Å^3 and the dipole moment is 2.19 D (ref 35). [f]Dipole moments from B3LYP/6-311+G**//B3LYP/6-31G* theory calculations. [g]N−H bond distance (Å) in protonated ion from B3LYP/6-31G* theory calculations.

for 3−5-ring compounds differ on average only by 0.3 ± 0.2 kcal/mol. Some or most of this difference may be due to computational artifacts or a shift in the NIST scales in this range. Because the computed values agree with experiment for aliphatic reference bases, we assigned the difference for the PANH proton affinities to computational artifacts for the large aromatic molecules, rather than a shift in the NIST scales.[20]

A possible source of computational artifact may be indicated by ionization energies (IEs). Tables 1 and 2 show both the computed PAs and IEs, and their difference from experiment, for 3−5-ring PANHs. Although the computed B3LYP PAs are too high by 3.9 ± 0.0.6 kcal/mol, the computed IEs are too low by a similar 5.6 ± 0.9 kcal/mol. We note that computationally, the energy of neutral M appears in both, with opposite signs, as PA = E(M) − E(MH$^+$) + E(H$^+$) and IE = E(M$^{+\bullet}$) − E(M). Therefore, the computed energies of the neutrals, E(M), affect both PA and IE, and the differences from experiment for both could be accommodated if the computed energies of the neutral bases, but not of the ions, are too high by 5 ± 1 kcal/mol. In comparison, similar level calculations on nonaromatic molecules in the companion paper gave very good agreement with experiment.[20]

This suggests that the B3LYP computations may underestimate the resonance stabilization of the large π systems, more in the neutral molecules than in the ions whose resonance stabilization is already reduced by protonation or ionization. Further, the computational effect can be somewhat larger in ionization, which reduces or eliminates the aromaticity of the π system in the M$^{+\bullet}$ ions, than in protonation of the N lone pair, which may affect less the aromaticity of the π system. For these reasons, the computational effect and difference from experiment can be somewhat larger on the IE than on the PA values as observed. With the M06-2X functional the PAs are too low by 0.85 ± 0.83 kcal/mol and the IEs are too high by 1.8 ± 0.7 kcal/mol, the opposite trend to that for the B3LYP functional. These observations suggest that the M06-2X functional deals better with resonance stabilization than does the B3LYP functional.

A further indication that the B3LYP proton affinities, but not the M06-2X and MP2 results, are related to size and aromaticity is that the difference of PA(M06-2X) − PA(experiment) is a constant −1.4 ± 0.9 kcal mol^{-1} for all our compounds with experimental PAs, and the MP2 results were also lower than experiment by a constant 2.7 ± 1.6 kcal mol^{-1} regardless of the

DOI: 10.1021/jp5069939
J. Phys. Chem. A 2015, 119, 127−139

number of aromatic rings. In comparison, the difference PA(B3LYP) − PA(experiment) increases from 0.2 kcal mol^{-1} for nonaromatic amines, to 1.5 kcal mol^{-1} (2 rings, pyridine); 2.5 kcal mol^{-1} (2 rings); and 3.9 kcal mol^{-1} (3−5 rings) PANHs, for both one-nitrogen and two-nitrogen compounds.

Although the results with the M06-2X reproduce the experimental PAs nearly within experimental uncertainty, the different results given by various methods suggest that computational methods for large aromatics and other compounds in the high GB/PA range need further studies.

The proton affinities in Table 1 correspond to 298 K and are higher only by about 0.6 kcal mol^{-1} than those at 0 K. The thermal corrections reflect the vibrational energy differences between $E(M)$ and $E(MH^+)$ at 0 K and 298 K, plus the contribution of $E(H^+)$ at 298 K (because $E(H^+) = 0$ at 0 K). Noting that PA = $E(M) + E(H^+) - E(MH^+)$ and that $(E(H^+)(298\ K) = 1.48$ kcal/mol, the vibrational energy effects in $E(M) - E(MH^+)$ without the $E(H^+)$ contribution would make PA(M)(0 K) − PA(M) (298 K) = 0.88 kcal/mol. These thermal corrections make only a small contribution to the PA(298 K) values, comparable to the experimental uncertainty. The largest M06-2X PA in Table 1, for dibenzo[*b*,*i*]acridine is 241.2 kcal mol^{-1} and the GB is 233.3 kcal mol^{-1}.

Table 1 also lists the values of protonation entropies or half reaction entropies,[33] defined as $\Delta S_{prot} = S°(BH^+) - S°(B)$ at 298 K, calculated at the B3LYP/6-31G* level of theory following geometry optimization. For our set of molecules, ΔS_{prot} ranges from 0.4 cal K^{-1} mol^{-1} for pyridine to 3.2 cal K^{-1} mol^{-1} for dibenzo[*c*,*h*]acridine. The mean value is 0.93 ± 0.55 cal K^{-1} mol^{-1} with the values for dibenzo[*a*,*c*]acridine, dibenzo[*f*,*h*]-quinoline, and especially dibenzo[*c*,*h*]acridine being outliers. The differences in ΔS_{prot} values may be attributed to differences in the vibrational contributions to the entropies $S(MH^+) - S(M)$. For dibenzo[*c*,*h*]acridine the vibrational contribution is 1.8 cal K^{-1} mol^{-1} whereas for dibenzo[*a*,*j*]acridine it is 0.6 cal K^{-1} mol^{-1}. The protonated ions with a relatively large positive protonation entropy (>1 K^{-1} mol^{-1}) have a common structural feature, where the protonating N−H hydrogen is close to a hydrogen on a ring two removed from the heterocyclic ring, which allows steric interaction of these hydrogens. For dibenzo[*a*,*c*]acridine the closest hydrogens are separated by 1.849 Å, and in dibenzo[*a*,*j*]acridine they are separated by 2.039 Å. The hydrogen−hydrogen steric repulsion upon protonation may cause out-of-plane twisting of the rings introducing low-frequency vibrations with a positive entropy term. Steric interactions in PAHs with bay regions, and the influence on the CH stretching frequencies have been discussed by Bauschlicher et al.[34]

The protonation entropy for the series of linear heterocyclics: pyridine, quinoline, benzo[*g*]quinoline, 1-azanaphthacene, and 1-azapentacene increases as the size of the molecule increases: 0.42 < 0.56 < 0.68 < 0.71 < 0.94 cal K^{-1} mol^{-1}. This also suggests that protonation increases the vibrational flexibilities of these rigid structures increasingly with increasing molecular size. Nevertheless, ΔS_{prot} of these magnitudes makes little contribution to GB as ΔS_{prot} of 1 cal K^{-1} mol^{-1} contributes 0.3 kcal mol^{-1} to GB at 298 K.

Even the exceptionally large ΔS_{prot} for a PANH, 3.2 cal/(mol K) for dibenzo[*c*,*h*]acridine, contributes only 0.96 kcal mol^{-1} to GB at 300 K. This effect may result as the proton attached to the central nitrogen repulses two end-ring hydrogens that are sterically close to it. This suggests that this protonated ion may be slightly twisted, but the calculated harmonic frequencies show that all the ions in this study are planar.

3b. Polarizabilities, Correlations with Proton Affinities, and Structural Effects. Table 3 lists the polarizabilities calculated at the B3LYP/6-31G* level, and also the dipole moments of the neutral molecules calculated at the B3LYP/6-311+G**//B3LYP/6-31G* level. For the molecules for which experimental values (pyridine, quinoline, and isoquinoline) are available, agreement with B3LYP/6-311+G**//B3LYP/6-31G* values are good and slightly better than the M06-2X/6-311+G**//B3LYP/6-31G* values (standard deviation of 0.10 versus 0.13). For this reason we feel justified in quoting the charges from B3LYP/6-311+G**//B3LYP/6-31G* calculations.

The dipole moments are mostly between 2 and 3 D. Because N carries the largest negative charge in these compounds, those with N near the center have small dipole moments, whereas with N at end positions they have the largest dipole moments.

The polarizabilities increase with molecular size. For the smaller species there is little variation between the polarizabilities of isomers. For isomers with a straight chain of rings like 1-azanaphthacene the polarizability is higher than for bent or more compact arrangements of rings like the azapyrenes. Correspondingly, the linear isomers also tend to have higher PAs than bent isomers (e.g., acridine vs phenanthridine).

Although the PAs increase with molecular size and polarizability, the NBO analysis below shows that in all the protonated $(PANH)H^+$ ions a nearly constant +0.43 charge from the full proton charge remains on the NH proton and therefore the +0.57 unit charge is transferred from the proton to the rest of the ion. The proton affinity then increases with size and polarizability not because more charge is delocalized from the proton as may be expected, but because the charge that is transferred to the rest of the ion is delocalized better in the more polarized ions.

Some further structural effects are also noted, for example, by comparing the three-ring compounds acridine, phenanthridine, and benzo[*h*]quinoline in Table 2. (PA_{exp} = 232.4, 228.5, 228.0; PA_{calc}(M06-2X) = 232.3, 228.4, 226.3 kcal/mol, respectively.) The PAs correlate with the computed polarizabilities, where acridine is the highest (22.2 Å^3) and phananthridine and benzo[*h*]quinoline are similar (20.9 and 21.1 Å^3, respectively). In acridine with the highest PA, the protonated N is in the central ring, and adjacent rings attached linearly on both sides allow the most efficient polarization by the positive charge. Phenanthridine also has N in the central ring, but the bent structure may allow less efficient overall polarization, whereas N in a peripheral ring as in benzo[*h*]quinoline may allow even less efficient interaction of the protonated end ring with the rest of the molecule, in particular, the furthest ring.

Figure 2 shows the calculated N_1 proton affinities as a function of the calculated polarizabilities for 31 compounds. The linear trendline has the form PA = 0.4077α + 224.22 kcal/mol, R^2 = 0.6992 and a standard deviation of 2.3 kcal mol^{-1} (α in Å^3). In either case, the proton affinity increases with polarizability as the ionic charge transferred from the proton can disperse better with increasing polarizability.

Deviations of PA from the linear regression line are shown in Table 3. Some of these deviations can be understood by considering how the ionic charge can be distributed over the molecule. Proton affinities larger than expected from the correlation are usually, but not always, associated with retention of more charge on the N-containing ring.

DOI: 10.1021/jp5069939
J. Phys. Chem. A 2015, 119, 127−139

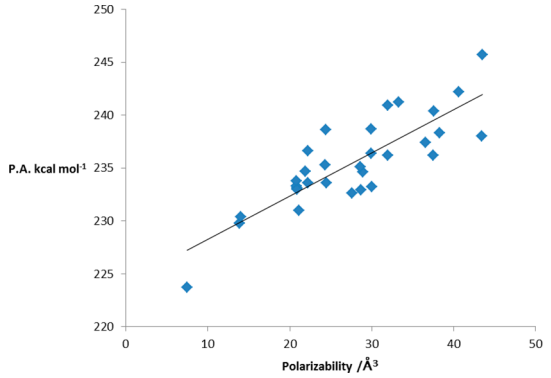

Figure 2. Proton affinity as a function of polarizability (α). Linear regression parameters: PA = 0.4077 α + 224.22 kcal/mol. α in Å^3, R^2 = 0.6992. All points are data from Table 1.

3c. Extrapolations to N-Doped Graphene. It would be of interest to extrapolate the PA data to infinite polarizability, corresponding to the PA of edge-N-doped graphene. For example, the PA of pure graphene, and the H atom affinity of ionized graphene, were estimated from variations with size in polycyclic aromatic hydrocarbons.[13] The present data do not allow direct extrapolations to N-doped graphene but suggest some limiting values and allow estimates for some PANH structural classes.

Extrapolating from the PANHs to N-doped graphene would be possible if the PAs would approach an asymptotic limit with increasing size or polarizability. However, PA keeps increasing linearly in Figure 2, suggesting that the PA will increase further with size and polarizability. The highest M06-2X/6-311+G**//B3LYP/6-31G* PA of the present compounds, 241.2 kcal mol^{-1}, then constitutes the lower limit of the PA of an infinite edge-N-doped graphene sheet.

The PA of an infinite size molecule can be estimated for a PANH subgroup, a linear chain of rings with N in one end ring, i.e., linear 1-Aza PANHs. A quartic fit to the proton affinities of these linear PANHs in Figure 3 for the series of pyridine,

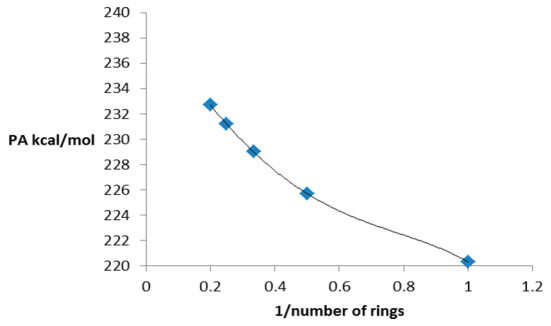

Figure 3. Proton affinity (M06-2X) as a function of 1/(number of rings) for linear end-ring-N heterocyclics with a N atom at the end of chain.

quinoline, 1-azaanthracene, 1-azanaphthacene, and 1-azapentacene as a function of $1/n$ (n = number of rings) gives a GB of 236.6 and a PA of 239.9 kcal mol^{-1} for protonating the nitrogen in the end ring (Figure 3). The quartic fit is PA = $19(1/n)^4$ + $22.4)(1/n)^3$ + $17.3(1/n)^2$ − $40.3(1/n)$ + 239.9, where n is the number of rings, giving PA = 239.9 kcal mol^{-1} for n = infinity, for the PA of an infinite linear chain 1-Aza-PANH molecule.

In comparison to linear PANHs protonated on an end ring, linear PANHs with N in the central ring are better analogues for an N-doped edge row of N-doped graphene. They have higher computed PAs than the 1-Aza PANHs. For example, the difference for the 3-ring linear compounds is PA(acridine) − PA(1-azaanthracene) = 3.3 kcal mol^{-1} and for the 5-ring compounds PA(dibenzo(b,i)acridine) − PA(1-azapentacene) = 8.5 kcal mol^{-1}. If these differences level off at infinite size, for example, to 15 kcal mol^{-1}, then the above lower limit PA > 241 kcal mol^{-1} for linear 1-Aza PANHs would predict PA > 256 kcal mol^{-1} for an infinite linear center-ring-N PANH molecule, making it into a gas-phase superbase.

This infinite linear center-N PANH chain can be increased to an edge-row-N-doped graphene sheet by adding a sheet of fused rings. The PA would then increase further with increasing size and polarizability. For example, from isoquinoline to 4-azapyrene the PA increases by 2.6 kcal mol^{-1}; from acridine to dibenzo(a,j)acridine, by 2.9 kcal mol^{-1}, and from quinoline to 1-azapyrene by 8.1 kcal mol^{-1}. The effect should decrease when fused rings are added to larger linear PANHs where the charge is already delocalized in the parent ion. Assuming a PA increase of 5 kcal mol^{-1} in going from an infinite linear center-ring-N PANH to an infinite edge-N-doped graphene sheet, the PA would increase from the above lower limit of >256 to a lower limit of >261 kcal mol^{-1}, making edge-N-doped graphene also a gas-phase superbase. Proceeding to edge-N-doped three-dimensional graphite the enthalpy of protonation should increase further, approaching the protonation enthalpy of 270−275 kcal mol^{-1} of a different condensed-phase system, liquid water.

These examples illustrate a method to estimate the protonation enthalpy of edge-N-doped graphene. Extending computations to still larger PANHs should show more clearly the trends with increasing molecular size and allow more accurate estimates for the protonation enthalpies of N-doped graphene and graphite.

3d. Atomic Charges: Protonated NH Group. Table 4 presents the charges calculated at the B3LYP/6-311+G**//B3LYP/6-31G* level of theory on the protonated N−H groups. Remarkably, the charges on H and N in the protonated N−H function remain nearly constant from pyridineH$^+$ to the largest ions, regardless of size, polarizability and proton affinity. The average charge on the N−H proton on all the ions is a nearly constant q(H) = 0.43 ± 0.01 units, and therefore the average charge transferred to the rest of the ion is 0.57 ± 0.01 for all the ions (because the total charge is unity). The protonated nitrogen has an average charge of q(N) = −0.46 ± 0.01 that is also nearly constant among the ions, and therefore the charge on the NH group q(H) + q(N) = −0.03 ± 0.02 is also constant nearly zero among the (PANH)H$^+$ ions. Because the ion carries a unit positive charge, the hydrocarbon C and H atoms carry a nearly full unit charge in all the ions.

These results are unexpected because the increasing proton affinities with polarizability suggests that more charge may delocalize from the proton to the hydrocarbon rings in the larger ions. However, the constant q(H) shows that the increasing proton affinities result not from increasing charge transfer from the proton, but from increasing dispersion of the transferred charge in the hydrocarbon parts of the ions. These effects are illustrated by Figure 4, which allows comparing the atomic charges in the neutral molecules and in the protonated ions, and by Figure 5 that shows changes in charge upon protonation in pyridine, quinoline, and acridine, and up to five-ring linear compounds.

Interestingly, the constant q(H) applies not only to the aromatic (PANH)H$^+$ ions, but for a range of various nitrogen

DOI: 10.1021/jp5069939
J. Phys. Chem. A 2015, 119, 127−139

Table 4. Atomic and Ring Charges on Protonated MH^+ Species[a]

		atomic charges[b]			ring charges[b,c]			
formula	molecule	qN[d]	qH[d]	A	B	C	D	E
C_5H_5N	pyridine	−0.44	0.44	0.559*				
C_9H_7N	quinoline	−0.44	0.43	0.362	0.207*			
	isoquinoline	−0.45	0.44	0.293	0.269*			
$C_{13}H_9N$	acridine	−0.46	0.42	0.346	−0.110*	0.346		
	benzo[g]quinoline	−0.45	0.43	0.216	0.197	0.160*		
	benzo[*f*]quinoline	−0.45	0.43	0.184	0.203	0.186*		
	benzo[*h*]quinoline	−0.45	0.43	0.179	0.198	0.196*		
	2-azaphenanthrene	−0.45	0.44	0.216	0.113	0.235*		
	phenanthridine	−0.44	0.43	0.263	0.228*	0.081		
	2-azaanthracene	−0.46	0.43	0.234	−0.004	0.213*		
	3-azaphenanthrene	−0.45	0.43	0.198	0.119	0.250*		
$C_{15}H_9N$	1-azapyrene	−0.47	0.42	0.187	0.160	0.225	0.005*	
	2-azapyrene	−0.44	0.43	0.174	0.124	0.116	0.153*	
	4-azapyrene	−0.44	0.43	0.210	0.117	0.021*	0.225	
$C_{17}H_{11}N$	1-azanaphthacene	−0.45	0.43	0.172	0.094	0.175	0.134*	
	α-naphthoquinoline	−0.47	0.42	0.207	0.184	−0.128*	0.207	
	benzo(*a*)acridine	−0.46	0.42	0.306	−0.114*	0.204	0.188	
	benzo(*c*)acridine	−0.46	0.42	0.314	−0.089*	0.181	0.177	
	naphtho(2,3-*h*)quinoline	−0.45	0.42	0.148	0.119	0.151	0.163*	
	dibenzo(*f*,*h*)quinoline	−0.45	0.43	0.151	0.170	0.065	0.190	
	4-azachrysene	−0.49	0.43	−0.167	0.029	0.303	0.408*	
	naphtho(2,1-*f*)quinoline	−0.44	0.43	0.151	0.062	0.212	0.149*	
	2-azachrysene	−0.45	0.43	0.132	0.086	0.113	0.236*	
$C_{19}H_{11}N$	10-azabenzo[*a*]pyrene	−0.47	0.42	0.165	0.101	0.207	0.126	−0.020*
$C_{21}H_{13}N$	1-azapentacene	−0.46	0.42	0.135	0.082	0.090	0.159	0.110
	dibenzo[*a*,*c*]acridine	−0.46	0.42	0.137	0.160	0.066	−0.078*	0.299
	dibenzo[*a*,*h*]acridine	−0.46	0.42	0.176	0.189	−0.118*	0.169	0.168
	dibenzo[*a*,*i*]acridine	−0.47	0.41	0.184	0.146	−0.091*	0.183	0.168
	dibenzo[*a*,*j*]acridine	−0.47	0.42	0.166	0.174	−0.096*	0.174	0.166
	dibenzo[*b*,*i*]acridine	−0.49	0.41	0.194	0.155	−0.107*	0.155	0.194
	dibenzo[*c*,*h*]acridine	−0.46	0.42	0.152	0.183	−0.086*	0.183	0.152

[a]Units of proton charge. [b]From B3LYP/6-311+G**//B3LYP/6-31G* calculations and NBO analysis. [c]Ring numbers starting with leftmost and topmost ring. Numbers marked with an asterisk designate the N-containing ring. When the charge on a ring is calculated, the charge on bridging atoms is shared equally with both or all three rings. [d]Charge on N and H of protonated nitrogen.

bases down to NH_4^+ where $q(H) = 0.488$ was found by 6-31G* Mulliken charge analysis,[36] suggesting also that $q(H)$ is not sensitive to the computational method.

This constant $q(H)$ for NH_4^+ and the $(PANH)H^+$ suggests that it may apply also in other nitrogen bases. As noted above, the variation of PA results then not from increasing charge transfer from NH protons to increasingly large ions, but from increasing dispersion of the charge, and the resulting decreasing Coulomb repulsion among partial positive charges on atoms of the hydrocarbon parts of the ions. We are examining these effects, and of nitrogen hybridization, on $q(H)$ and $q(N)$ in other, aliphatic protonated nitrogen bases.

Although $q(H)$ may be nearly constant in the protonated N bases, it can be changed by solvation. Hydrogen bonding to H_2O molecules usually makes the bonding proton more positive, and some positive charge is transferred from the ion to the solvent, although about 80% of the charge is retained by NH_4^+ even in bulk solution.[36−38] It would be of interest to learn how much charge is retained by alkylammonium and $(PANH)H^+$ ions in bulk solvation.

Similar to the $q(H)$ being constant, the N−H bond lengths in the $(PANH)H^+$ ions in Table 3 are also constant at 1.014−1.016 Å. Again, similar N−H bond lengths of 1.013 Å were found also in the NH_4^+ ion.[24] These features are consistent with N−H bonds in protonated nitrogen bases that are essentially covalent bonds.[39]

3e. Ring Charges. Table 4 above lists the charges on each ring in the protonated species, calculated using NBO atomic charges (ring A is the left-most/upper-most ring in Figure 1) from B3LYP/6-311+G**//B3LYP/6-31G* calculations. In calculating the charge on a ring, the charge on bridging atoms is shared by both or all three rings equally. The negative charge on N is included in the ring charges and the total (rings + protic H) charges add up to the +1 ionic charge in each ion.

In $pyridineH^+$, $quinolineH^+$, and $isoquinolineH^+$ the rings with protonated nitrogen have positive overall charges, even including the negative charge on nitrogen. However, in $acridineH^+$ the central ring that contains N is negative, which stabilizes the positive charges on the two side rings. Similarly in larger compounds, for example, in the dibenzoacridines (except the strongly asymmetrical dibenzo(*a*,*c*)acridine) where the N-bearing central ring is surrounded by two hydrocarbon rings on both sides, the positive charge is distributed about evenly on the hydrocarbon rings and stabilized by the negative central ring.

In contrast, when the protonated nitrogen is in the end rings, such as $quinolineH^+$, $isoquinolineH^+$, the $benzoquinolinesH^+$, $2\text{-}azaphenanthreneH^+$, $3\text{-}azaphenanthreneH^+$, dibenzo(*f*,*h*)-$quinolineH^+$, $2\text{-}azachryseneH^+$, $azapentaceneH^+$, and the

DOI: 10.1021/jp5069939
J. Phys. Chem. A 2015, 119, 127−139

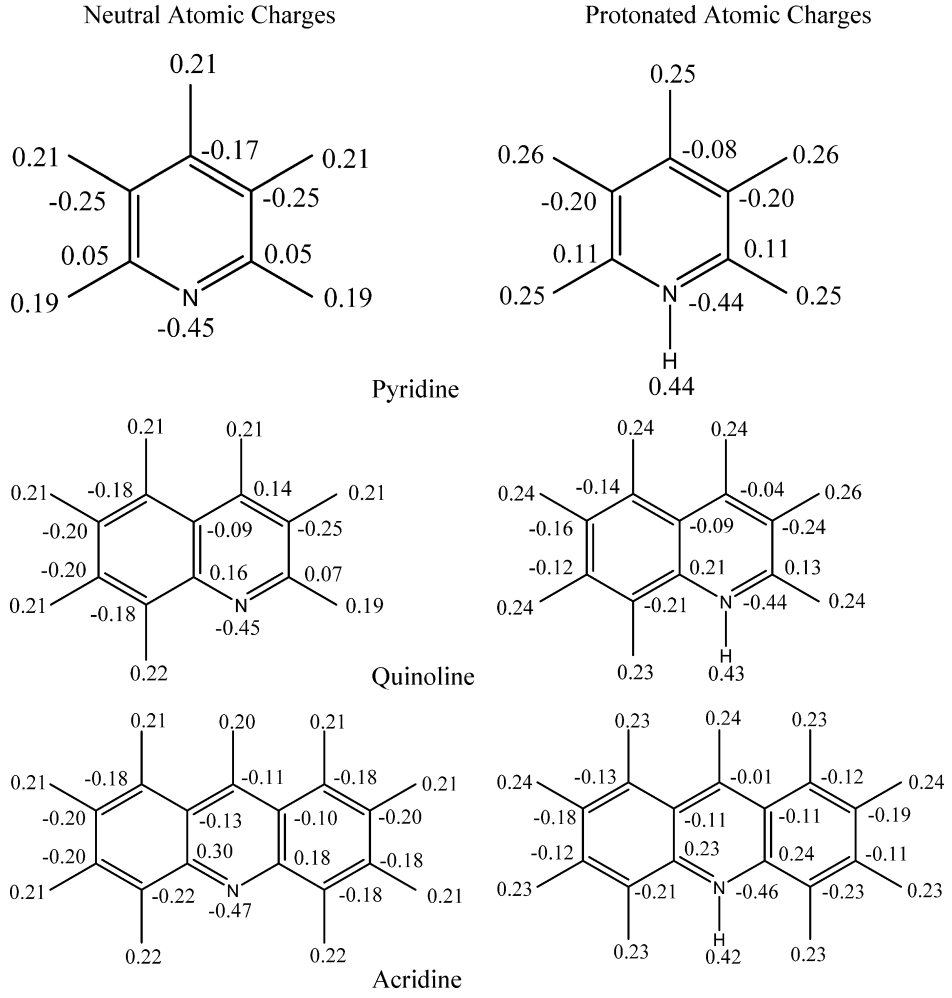

Figure 4. Atomic charges in neutral and protonated PANHs (units of proton charge).

compact protonated azapyrenes, the positive charge is distributed more evenly among the rings and all the rings have an overall positive charge. 4-AzachryseneH$^+$ is an exception to this rule.

3f. Atomic Charges and Changes upon Protonation. As discussed above, the atomic charges q(H) and q(N) on the NH group are effectively constant among the ions, and the charge transferred to the C and other H atoms are distributed more diffusely with increasing size. Comparing pyridineH$^+$, quinolineH$^+$, and acridineH$^+$, the q(H) in the para position to N remains effectively constant, and decreases slightly on the side ring hydrogens in that order. The charges on the para C atoms are affected more strongly, from −0.08 to −0.04 to −0.01, respectively.

Figure 5 shows the changes in atomic charges upon protonation. First, the changes of q(H) (from +1 in the separated proton) are effectively equal among the ions; i.e., the charge remaining on the proton is equal in all the ions as discussed above. Remarkably, q(N) is also constant, not only in all the ions but also in the neutral bases; i.e., it remains nearly unchanged by protonation. Further, the increase in q(para C) upon protonation is a constant 0.10 units from the 2-ring to the 5-ring ions.

Figure 5 and Table 5 show changes in ring charges upon protonation. The largest changes in atomic charges upon protonation, other than the N-containing ring, are on the ring furthest from the N-containing ring. There is more charge on this ring when the chain is bent away from the N atom, for example, in benzo[f]quinoline as compared with benzo[h]quinoline. These charge distributions may minimize the Coulombic repulsion between the positive charge on the protonated ring and the positive charge in the rest of the ion.

However, in some positions protonation affects the atomic charges less with increasing distance from the protonated center. For example, in the end-ring-protonated 2−5-ring ions in Figure 4, the "para" C and H atoms have decreasing charge changes as the rings are increasingly remote form the protonated end-ring.

Overall, the protonation effects on atomic charges are increasingly more distributed with increasing size. Consequently, the total Coulomb repulsion among the added charges upon protonation decreases with increasing size, making protonation more exothermic with increasing size and polarizability and leading to increasing PAs as observed.

As to structural effects, for the dibenzoacridines the charge on the furthest ring(s) from the N-containing ring correlates with the proton affinities. The charge on the furthest ring is greater for straight chains of rings and this also correlates with a higher proton affinity. For example, in the 3-ring compounds, the linear acridine has a higher PA than the bent phenanthridine, and in the 4-ring compounds, the linear α-naphthoquinoline (i.e., benzo(b)acridine) has a higher proton affinity than the bent benzo(a)acridine and benzo(c)acridine. These effects are caused

DOI: 10.1021/jp5069939
J. Phys. Chem. A 2015, 119, 127−139

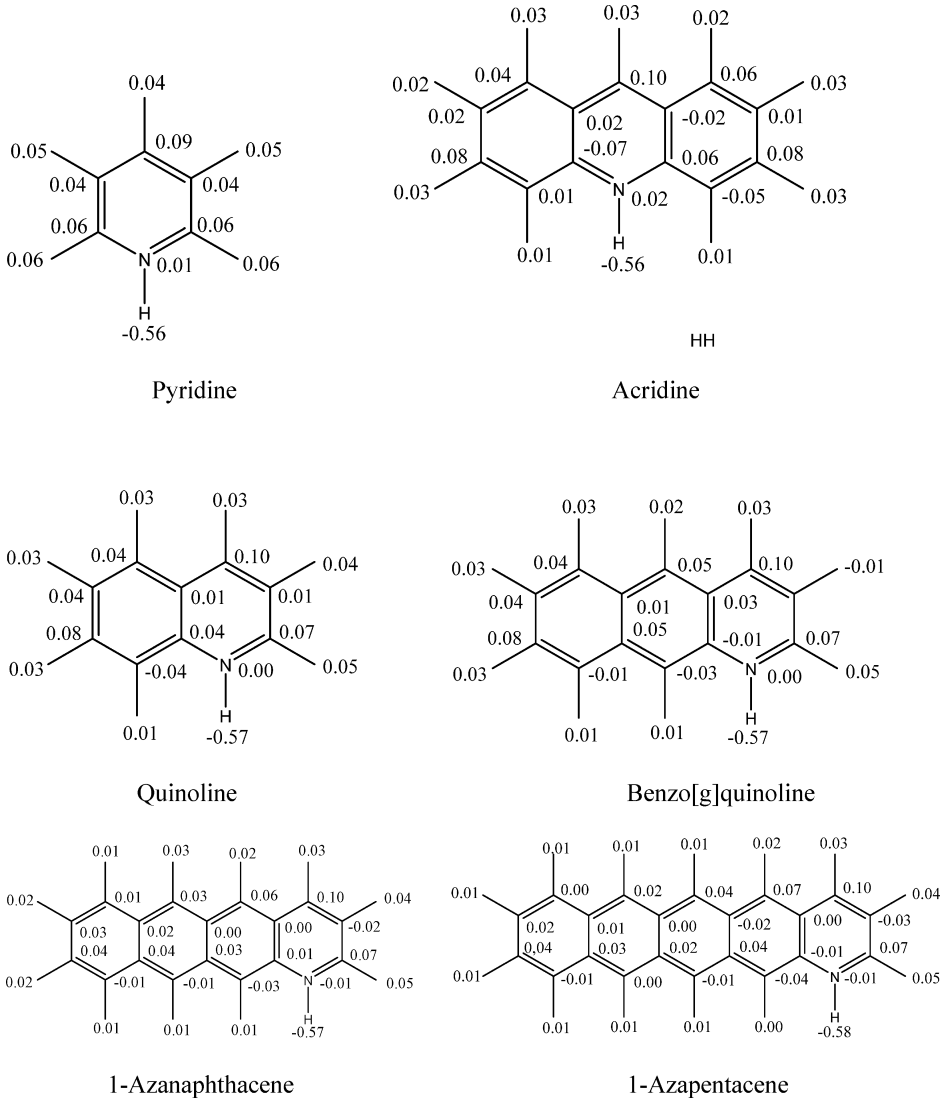

Figure 5. Changes in atomic charges upon protonation of linear nitrogen heterocyclics (units of proton charge).

by factors other than charge delocalization from the N-containing ring, because there appears to be no relationship between the charge on that ring and the proton affinity.

4. MUTUAL EFFECTS OF RING NITROGENS IN AROMATIC DIAZINES

Introducing a second nitrogen leads to many possible isomers, ten in two-ring two-nitrogen compounds alone. This allows various interactions between the two nitrogens depending on their positions and separation and on their interactions with the rest of the molecule.

In the one-nitrogen compounds above we observed effects of molecular size and polarizabilty on the proton affinities. We shall examine here the effects of size and polarizability on the interactions between two ring nitrogens.

First, in the 1-ring diazines, introducing a second ring nitrogen into pyridine decreases the M06-2X/6-311+G**//B3LYP/6-31G* proton affinity of the 1,2-, 1,3-, to 1,4-diazines (pyridazine, pyrimidine, and pyrazine), by 3.7, 10.5, and 13.5 kcal/mol, respectively. Similarly, in 2-ring compounds, a second nitrogen can be added to the N-containing ring of quinoline, leading to 1,2-, 1,3-, and 1,4-naphthyridine (cinnoline, quinazoline, and quinoxaline, respectively), which decreases the PA by 2.9 (at N1), 7.8, and 11.7 kcal/mol, respectively (Table 1). The absolute reduction is smaller in the 2-ring than in the 1-ring compounds. The reduced effect may be due to the more delocalized charge in the 2-ring compounds, which can make the redistribution of charge by the second nitrogen less effective.

Specifically, protonating a ring nitrogen makes that N−H group more positive, creating increasing repulsion with the $C^{\delta+}-N^{\delta-}-C^{\delta+}$ dipole of the other nitrogen. This repulsion in the ion can account for the reduction of the PA by the second nitrogen, in the order 1,2 < 1,3 < 1,4 as the $C^{\delta+}-N^{\delta-}-C^{\delta+}$ dipole is increasing better aligned to repulse the new positive N−H group formed by protonation of the first nitrogen. Also, the effect will be smaller in the larger ions, as observed, where the charges are more diffuse. This accounts qualitatively for the relative proton affinities of 1-ring and 2-ring compounds where both nitrogens are on one ring.

A second series in diazines also concerns compounds where the two nitrogens are in one ring. In this series, the second nitrogen is introduced para to the first nitrogen in the same ring in 1-ring, 2-ring, or 3-ring diazines, going from pyridine to 1,4-diazine, from quinoline to 1,4-naphthyridine, and from acridine to phenazine, respectively. These para N substitutions decrease the PA by 13.5, 11.7, and 10.4 kcal/mol, respectively (Table 1).

DOI: 10.1021/jp5069939
J. Phys. Chem. A 2015, 119, 127−139

Table 5. Change of Ring Charges on Protonation[a]

		change in ring charges[b]				
formula	molecule	A	B	C	D	E
C_5H_5N	pyridine	0.559*				
C_9H_7N	quinoline	0.241	0.328*			
	isoquinoline	0.267	0.295*			
$C_{13}H_9N$	acridine	0.217	0.147*	0.217		
	benzo[*g*]quinoline	0.201	0.090	0.282*		
	benzo[*f*]quinoline	0.158	0.096	0.319*		
	benzo[*h*]quinoline	0.133	0.136	0.304*		
	2-azaphenanthrene	0.174	0.121	0.235*		
	phenanthradine	−0.045	0.388*	0.229		
	2-azaanthracene	0.202	0.123	0.242*		
	3-azaphenanthrene	0.158	0.123	0.285*		
$C_{15}H_9N$	1-azapyrene	0.167	0.145	0.100	0.166*	
	2-azapyrene	0.750	0.124	0.102	0.172*	
	4-azapyrene	0.197	0.110	0.135*	0.130	
$C_{17}H_{11}N$	1-azanaphthacene	0.161	0.087	0.072	0.255*	
	α-naphthoquinoline	0.193	0.197	0.121*	0.073	
	benzo(*a*)acridine	0.183	0.122*	0.306	0.169	
	benzo(*c*)acridine	0.188	0.166*	0.110	0.118	
	naphtho(2,3-*h*)quinoline	0.288	0.107	0.163	0.018*	
	dibenzo(*f*,*h*)quinolone	0.139	0.088	0.036	0.313*	
	4-azachrysene	0.144	0.211	0.075	0.127*	
	naphtho(2,1-*f*)quinoline	0.283	0.088	0.075	−0.127*	
	2-azachrysene	0.251	0.117	0.065	0.133*	
$C_{19}H_{11}N$	10-azabenzo[*a*]pyrene	0.162	0.085	0.063	0.126	0.144*
$C_{21}H_{13}N$	1-azapentacene	0.132	0.073	0.075	0.064	0.232*
	dibenzo[*a*,*c*]acridine	0.139	0.240	−0.336	0.156*	0.384
	dibenzo[*a*,*h*]acridine	0.160	0.087	0.149*	0.070	0.117
	dibenzo[*a*,*i*]acridine	0.167	0.043	0.152*	0.059	0.316
	dibenzo[*a*,*j*]acridine	0.149	0.074	0.138*	0.074	0.149
	dibenzo[*b*,*i*]acridine	0.180	0.041	−0.184*	0.041	0.180
	dibenzo[*c*,*h*]acridine	0.107	0.103	0.162*	0.103	0.107

[a]From B3LYP/6-311+G**//B3LYP/6-31G* calculations and NBO analysis. Units of proton charge. [b]Ring numbers starting with leftmost and topmost ring. Numbers with asterisks designate the N-containing ring. In calculating the charge on a ring, the charge on bridging atoms is shared equally with both or all three rings.

Again, the effects are smaller with increasing molecular size where the charge is increasingly delocalized from the nitrogen-bearing ring, which decreases the repulsive charge−dipole interactions caused by protonation.

Finally, the effects of a second nitrogen can be compared when it is added in the same ring as the first nitrogen or in a different ring. In 2-ring compounds, adding a second nitrogen in the nitrogen-bearing ring in the para position, from quinoline to quinoxaline, decreases the computed PA by 11.7 kcal/mol, whereas adding N to the second ring in a "pseudo-para" position forming 1,5-naphthyridine decreases the PA by 5.8 kcal/mol, and adding the second nitrogen in a proximate "ortho" position (in quinazoline) to the first nitrogen decreases the PA by 7.8 kcal/mol. The effects of introducing nitrogen in the second ring are smaller than introducing it in the first ring, and the effect in the "para"-like position is larger than in the "ortho"-like position, in line with the above-noted charge−dipole interactions in the ions.

The mutual effects of two ring nitrogens were studied theoretically for the diazines, but more such studies are needed, for example, for the interactions of nitrogens in different rings in larger PANHs. We are continuing to investigate experimentally and theoretically such mutual effects in isomeric PANHs in a larger series of compounds.

5. CONCLUSIONS

Molecular size, polarizability, and geometry all affect significantly the proton affinities of aromatic nitrogen heterocyclic compounds. Similar to other nitrogen and oxygen bases, the proton affinities and gas-phase basicities generally increase with molecular size and polarizability, subject to structural effects depending on the position of the basic nitrogen atom in the conjugated ring system. These effects could reflect increased delocalization of the charge from the proton to increasingly more polarizable PANH molecules. However, NBO analysis shows that the charge on the proton remains nearly constant, and the overall charge on the N−H group is nearly zero, independent of molecular size and proton affinity. Therefore, a nearly full unit positive charge is located on the hydrocarbon C and H atoms of the ions. The increasing proton affinity results from increasing delocalization of this charge with the increasing polarizabilities of the ions.

The PA increases linearly with molecular polarizabilities in the studied compounds and does not level off asymptotically toward a constant value, preventing direct extrapolation to the PA of edge-N-doped graphene. However, the PA of a linear chain of rings with one N on the central ring extrapolates to about 250 kcal/mol for an infinite chain. The PA should be even higher for a two-dimensional planar, more polarizable edge-N-doped gra-

DOI: 10.1021/jp5069939
J. Phys. Chem. A 2015, 119, 127−139

phene sheet. Although our compounds are not superbases (their PA < 250 kcal mol^{-1}), the results suggest that an edge-N-doped graphene sheet may be a superbase.

In two-nitrogen compounds, charge delocalization in larger molecules weakens the mutual effects of the nitrogens that decrease the proton affinities. These effects depend on the mutual positions of the nitrogens and their location in the molecule.

Some matters requiring further examination include:

- The absolute PAs of other PANHs above 230 kcal/mol determined from theory, compared with measurements referenced to thermochemical ladders extrapolated from lower PA compounds. The differences between theory and experiment may be due to computational artifacts or a shift in the experimental PAs in the high range.
- The variation of q(H) in various types of protonated nitrogen bases.
- The effects of several ring nitrogens and their mutual interactions on the basicities of multinitrogen and multiring PANHs.
- In solvated systems, the effects of stepwise and bulk solvation on the atomic charges. How does the solvation of the protonated nitrogen groups and of the alkyl or aromatic substituents affect each other, and how much charge the various (PANH)H$^+$ ions retain in solution.
- Extrapolations from (PANH)H$^+$ ions to protonated edge-N-doped graphene.

These questions are important fundamentally and are useful in molecular simulations. We are conducting further work to address these subjects.

■ ASSOCIATED CONTENT

Supporting Information

Details of the charges on the rings of unprotonated PANH species are given. This material is available free of charge via the Internet at http://pubs.acs.org

■ AUTHOR INFORMATION

Corresponding Author

*R. G. A. R. Maclagan. Fax: (+64)3 364-2110. Phone: (+64)3 359-2915. E-mail: Robert.maclagan@canterbury.ac.nz.

Notes

The authors declare no competing financial interest.

■ ACKNOWLEDGMENTS

S.G. acknowledges the National Science Foundation for support (CHE-1300817).

■ REFERENCES

(1) Hayatsu, R.; Matsuoka, S.; Scott, R. G.; Studier, M. H.; Anders, E. Origin of Organic Matter in the Early Solar System-VII. The Organic Polymer in Carbonaceous Chondrites. *Geochim. Cosmochim. Acta* **1977**, *41*, 1325−1339.

(2) Hayatsu, R.; Anders, E. Organic Compounds inMeteorites and Their Origins. *Top. Curr. Chem.* **1981**, *99*, 1−37.

(3) Basile, B. P.; Middleditch, B. S.; Oró, J. Polycyclic Aromatic Hydrocarbons in the Murchison Meteorite. *Org. Geochem.* **1984**, *5*, 211−216.

(4) Hudgins, D. M.; Bauschlicher, C. W.; Allamandola, L. J. Variations in the Peak Positions of the 2.1 Micrometer Interstellar Emission Feature: A Tracer of N in the Interstellar Polycyclic Aromatic Hydrocarbon Population. *Astrophys. J.* **2005**, *632*, 316−332.

(5) Tielens, A. G. G. M. Interstellar Polycyclic Aromatic Hydrocarbon Molecules. *Annu. Rev. Astron. Astrophys.* **2008**, *46*, 289−337.

(6) Elsila, J. E.; Hammond, M. R.; Bernstein, M. P.; Sandford, S. A.; Zare, R. N. UV Photolysis of Quinoline in Interstellar Ice Analogues. *Meteorit. Planet. Sci.* **2006**, *41*, 785−796.

(7) Mattioda, A. L.; Hudgins, D. M.; Bauschlicher, C. W., Jr.; Rosi, M.; Allamandola, L. J. Infrared Spectroscopy of Matrix-Isolated Polycyclic Aromatic Compounds and Their Ions. 6. Polycyclic Aromatic Nitrogen Heterocycles. *J. Phys. Chem. A* **2003**, *107*, 1486−1498.

(8) Boersma, C.; Bregman, J. D.; Allamandola, L. J. Properties of Polycyclic Aromatic Hydrocarbons in the Northwest Photon Dominated Region of NGC 7023. I PAH Size, Charge, Composition, and Structure Distribution. *Astrophys. J.* **2013**, *769*, 117.

(9) El-Shall, M. S.; Daly, G. M.; Yu, Z.; Meot-Ner (Mautner), M. Comparative Polymerization in the Gas Phase and in Clusters. 2. Electron Impact and Multiphoton-Induced Reactions in Isobutene and Benzene/Isobutene Clusters. *J. Am. Chem. Soc.* **1995**, *117*, 7744−7752.

(10) Meot-Ner (Mautner), M.; Pithawalla, Y. B.; Gao, J.; El-Shall, M. S. Coupled Reactions of Condensation and Charge Transfer. 1. Formation of Olefin Dimer Ions in Reactions with Ionized Aromatics. Gas-Phase Studies. *J. Am. Chem. Soc.* **1997**, *119*, 8332−8341.

(11) Pithawalla, Y. B.; Meot-Ner (Mautner), M.; Gao, J.; El-Shall, M. S.; Baranov, V. I.; Bohme, D. K. Gas-Phase Oligomerization of Propene Initiated by Benzene Radical Cation. *J. Phys. Chem. A* **2001**, *105*, 3908−3916.

(12) Meot-Ner (Mautner), M. Ion Thermochemistry of Low-Volatility Compounds in the Gas Phase. 2. Intrinsic Basicities and Hydrogen-Bonded Dimers of Nitrogen Heterocyclics and Nucleic bases. *J. Am. Chem. Soc.* **1979**, *101*, 2396−2403.

(13) Meot-Ner (Mautner), M. Ion Thermochemistry of Low-Volatility Compounds in the Gas Phase. 3. Polycyclic Aromatics: Ionization Energies, Proton and Hydrogen Affinities. Extrapolations to Graphite. *J. Phys. Chem.* **1980**, *84*, 2716−2723.

(14) Aue, D. H.; Webb, H. M.; Bowers, M. T.; Liotta, C. L.; Alexander, C. J.; Hopkins, H. P. A Quantitative Comparison of Gas- and Solution-Phase Basicities of Substituted Pyridines. *J. Am. Chem. Soc.* **1976**, *98*, 854−856.

(15) Aue, D. H.; Webb, M. M.; Davidson, W. R.; Toure, P.; Hopkins, J. R.; Moulik, S. P.; Jahagirdar, D. V. Relationships Between the Thermodynamics and Protonation in the Gas Phase and Aqueous Phase for 2-, 3-, and 4-Substituted Pyrdines. *J. Am. Chem. Soc.* **1991**, *113*, 1770.

(16) Taft, R. W. Protonic Acidities and Basicities in the Gas Phase and in Solution: Substituent and Solvent Effects. *Prog. Phys. Org. Chem.* **1983**, *14*, 247−350.

(17) Taft, R. W.; Anvia, F.; Taagepera, M.; Catalan, J.; Elguero, J. Electrostatic Proximity Effects in the Relative Basicities and Acidities of Pyrazole, Imidazole, Pyridazine, and Pyrimidine. *J. Am. Chem. Soc.* **1986**, *108*, 3237−3239.

(18) Hunter, E. P. L.; Lias, S. G. Evaluated Gas Phase Basicities and Proton Affinities of Molecules: An Update. *J. Phys. Chem. Ref. Data* **1998**, *27*, 413−656.

(19) Hunter, E. P.; Lias, S. G. Proton Affinity Evaluation. In *NIST Chemistry WebBook*; NIST Standard Reference Database Number 69; Linstrom, P. J., Mallard, W. G., Eds.; National Institute of Standards and Technology: Gaithersburg, MD, 20899, http://webbook.nist.gov (retrieved July 8, 2014).

(20) Wiseman, A.; Sims, L. A.; Snead, R.; Gronert, S.; Maclagan, R. G. A. R.; Meot-Ner (Mautner), M. Protonation Energies of 1−5-Ring Polycyclic Aromatic Nitrogen Heterocyclics: Comparing Experiment and Theory. *J. Phys. Chem. A* **2014**, DOI: 10.1021/jp506913r.

(21) Evaluated PA of pyridine PA 222.2(0.4) kcal/mol from refs 18 and 19, based on 222.2, 222.8, 222.2, and 221.8 kcal/mol in refs 14−17.

(22) PAs of quinoline, isoquinoline and acridine from ref 15.

(23) Aue, D. H.; Webb, H. M.; Bowers, M. T. Quantitative Proton Affinities, Ionization Potentials, and Hydrogen Affinities of Alkylamines. *J. Am. Chem. Soc.* **1976**, *98*, 311−317.

(24) Aue, D. H.; Webb, H. M.; Bowers, M. T.; Liotta, C. L.; Alexander, C. J.; Hopkins, H. P. A Quantitative Comparison of Gas- and Solution-

DOI: 10.1021/jp5069939
J. Phys. Chem. A 2015, 119, 127−139

Phase Basicities of Substituted Pyridines. *J. Am. Chem. Soc.* **1976**, *98*, 854−856.
(25) Davidson, W. R.; Sunner, J.; Kebarle, P. Hydrogen Bonding of Water to Onium Ions. Hydration of Substituted Pyridinium Ions and Related Systems. *J. Am. Chem. Soc.* **1979**, *101*, 1675−1680.
(26) Lau, Y. K.; Saluja, P.P. S.; Kebarle, P.; Alder, R. W. Gas-Phase Basicities of N-methyl Substituted 1,8-Diaminonaphthalenes and Related Compounds. *J. Am. Chem. Soc.* **1978**, *100*, 7328−7334.
(27) Taagepera, M.; Brownlee, R. T. C.; Beauchamp, J. L.; Holtz, D.; Taft, R. W. Gas Phase Basicities and Pyridine Substituent Effects. *J. Am. Chem. Soc.* **1972**, *94*, 1369−1370.
(28) Curtiss, L. A.; Redfern, P. C.; Ragavachari, K.; Pople, J. A. Assessment of Gaussian-2 and Density Functional Theories for the Computation of Ionization Potentials and Electron Affinities. *J. Chem. Phys.* **1998**, *109*, 42−55.
(29) Baboul, A. G.; Curtiss, L. A.; Redfern, P. C.; Raghavachari, K. K.Gaussian-3 Theory Using Density Functional Geometries and Zero-Point Energies. *J. Chem. Phys.* **1999**, *110*, 7650−7657.
(30) Burk, P.; Koppel, I. A.; Koppel, I.; Leito, I.; Travnikov, O. Critical Test of Performance of B3LYP functional for Prediction of Gas-Phase Acidities and Basicities. *Chem. Phys. Lett.* **2000**, *323*, 482−489.
(31) Koppel, I. A.; Schwesinger, R.; Breuer, T.; Burk, P.; Herodes, K.; Koppel, I.; Leito, I.; Mishima, M. Intrinsic Basicities of Phosphorus Imines and Ylides: A Theoretical Study. *J. Phys. Chem. A* **2001**, *105*, 9575−9586.
(32) Kaljurand, I.; Koppel, I. A.; Kütt, A.; Rõõm, E.-I.; Rodima, T.; Koppel, I.; Mishima, M.; Leito, I. Experimental Gas-Phase Basicity Scale of Superbasic Phosphazenes. *J. Phys. Chem. A* **2007**, *111*, 1245−1250.
(33) East, A. L. L.; Smith, B. J.; Radom, L. Entropies and Free Energies of Protonation and Proton-Transfer Reactions. *J. Am. Chem. Soc.* **1997**, *119*, 9014−9020.
(34) Bauschlicher, C. W.; Peeters, E.; Allamandola, L. J. The Infrared spectra of Very Large Irregular Polycyclic Aromatic Hydrocarbons (PAHs): Observational Probes of Astronomical PAH Geometry, Size and Charge. *Astrophys. J.* **2009**, *697*, 311−327.
(35) Nelson, R. D.; Lide, D. R.; Maryott, A. A. Selected Values of Electric Dipole Moments for Molecules in the Gas Phase *Natl. Stand. Ref. Data Ser. (U. S., Natl. Bur. Stand.)* **1967**, *NBS 10*.
(36) Deakyne, C. A. Filling of Solvent Shells about Ions: Isomeric Clusters of $(H_2O)_nNH_3H^+$. *J. Phys. Chem.* **1986**, *90*, 6625−6623.
(37) Houriez, C.; Meot-Ner (Mautner), M.; Masella, M. Simulated Solvation of Organic Ions: Protonated Methylamines in Water Nanoproplets. Converegence Toward Bulk Properties and the Absolut Proton Solvation Enthalpy. *J. Phys. Chem. B* **2014**, *118*, 6222−6233.
(38) Zhao, Y. L.; Meot-Ner (Mautner), M.; Gonzalez, C. Ionic Hydrogen-Bond Networks and Ion Solvation. 1. An Efficient Monte Carlo/Quantum Mechanical Method for Structural Search and Energy Computations: Ammonium/Water. *J. Phys. Chem. A* **2009**, *113*, 2967−2974.
(39) Del Bene, J. E. A Molecular Orbital Study of Protonation. 2. Pyridine and the Diazines. *J. Am. Chem. Soc.* **1977**, *99*, 3617−3619.

DOI: 10.1021/jp5069939
J. Phys. Chem. A 2015, 119, 127−139